jet INTL JOURNAL OF ELECTRONICS AND TELECOMMUNICATIONS, 2025, VOL. 71, NO. 2, PP. 403-412
Manuscript received March 31, 2025; revised May, 2025. doi: 110.24425/ijet.2025.153586

Evaluation and experimental optimization of cheap ultrasonic acoustic linear position sensor

Maciej Zakrzewski, and Maciej Ławryńczuk

***Abstract*—This work is concerned with the adequate selection, evaluation and experimental optimization of a low-cost position sensor in an electromechanical system. The objective is to choose a sensor that satisfies the following criteria: it is very fast, provides accurate measurement, and is relatively inexpensive. Various distance measurement technologies, including vision, laser, acoustic, and touch sensors, have been evaluated. Ultrasonic sensors deliver the best performance in terms of cost-effectiveness and applicability. The developed system undergoes static and dynamic testing, with structural, environmental, and software adjustments improving measurement accuracy. The research significantly reduces measurement errors and enhances result repeatability. The article discusses challenges associated with ultrasonic sensors, such as acoustic resonances and environmental influences, and proposes mitigation strategies. The findings highlight the extensive potential of the system for various industrial and educational applications.**

***Keywords*—distance measurement; ultrasonic sensors; low-cost sensors; sensor optimization**

I. Introduction

THE role of laboratory classes in engineering studies is huge [1]. We cannot imagine a successful engineering education without sufficient laboratory hours. Laboratory tasks illustrate how theoretical concepts discussed during lectures work and inspire students to perform their experiments. Therefore, the appropriate selection of laboratory processes is of great importance. In the case of automatic control university education, we typically use classical laboratory stands, such as water tanks, pendulums, inverted pendulums, water tanks and magnetic levitation systems. They can be purchased from reliable firms with extensive experience developing interesting laboratory systems. Let us name Bytronic [2], Inteco [3] and Quanser [4]. In addition, we can observe that more and more laboratory stands are being designed and developed at universities. The AutomationShield is a great example. It is an open-source hardware and software initiative for control engineering education [5], [6] that includes, among others, magnetic levitation [7], floating ball, optical system, motor speed and position and other systems. Other examples of custom processes are the air levitation laboratory stand [8], the Furuta inverted pendulum [9], the thermal heating-ventilation process [10] and the ball-on-plate process [11]. Importantly, experiences with real laboratory devices give much better education than relying on virtual laboratories [12], [13]. We observe an important tendency to minimize costs necessary to develop custom-made laboratory devices aimed at the education of engineering students [6], [8]–[11], [14], [15].

Authors are with Institute of Control and Computation Engineering, Faculty of Electronics and Information Technology, Warsaw University of Technology, Warsaw, Poland (maciej.zakrzewski@pw.edu.pl, maciej.lawrynczuk@pw.edu.pl).

The authors of this study, as scientists deeply engaged in activities aimed at improving the quality of education for future scientific personnel and professionals entering the workforce, set themselves the goal of creating a new, innovative, engaging, and ambitious research platform. This platform is envisioned as a starting point for future work on advanced processes in the broadly understood fields of automation and robotics. The newly designed platform is intended to utilize and control magnetic phenomena to set the velocity and direction of motion for controlled objects. An ideal candidate for generating the magnetic field is an array of electromagnets, while a steel ball is perfectly suited as the regulated object.

During work on a setup designed for identifying and controlling a ball's direction and rolling speed using an array of electromagnets, a significant challenge has been encountered: the ball positioning system. This system must not only be precise but also extremely fast. Both of these attributes are critically important due to the high variability of the force generated by the magnetic field of a coil as a function of the distance from the axis of the electromagnet. Naturally, it is easy to imagine meeting these stringent requirements through very expensive, off-the-shelf or custom-designed solutions. However, this project set an additional ambitious constraint: low cost. The key question thus became whether it is possible to measure distance quickly, accurately, and affordably without compromising by selecting at most two of these three characteristics.

This work takes on the challenge of fast and cost-effective positioning. Adequate selection, evaluation and experimental optimization of a low-cost position sensor in an electromechanical system are thoroughly discussed. We aim to find a sensor that satisfies the following criteria: it is very fast, provides accurate measurement, and is relatively inexpensive. A great variety of sensors are available on the market. However, without a proper optimization thoroughly detailed in this work, achieving the required measurement accuracy within the assumed time is impossible. The laboratory process considered is an electromechanical system comprised of a set of electromagnets that move a ball. Importantly, fast, inexpensive, precise distance measurement has applications in many industrial sectors. In particular, fast and efficient distance sensors are necessary for numerous automatic control and robotics applications. Expensive solutions only become relevant when affordable options prove inadequate. Therefore, this study reviews available solutions and evaluates their suitability.

This work consists of the following parts:

- Section II presents process description and laboratory setup, starting from the conceptual process schematic, technical assumptions and the hardware and software realization.
- Section III reviews possible approaches to position measurements, i.e., vision distance detectors, laser distance detectors or acoustic distance sensors. In addition to technical features and price, the advantages and disadvantages of the solutions discussed are presented.
- Section V describes the process of an adequate selection, practical evaluation and optimization of acoustic distance sensors for the developed laboratory process. An array of experimental methods that improve measurement accuracy and efficiency are thoroughly discussed, e.g., sidewall optimization or shape and sizes comparison.
- Section VI summarizes the article and points out the obtained results.

II. Process Description and Laboratory Setup

As the Introduction mentions, the presented research results are crucial to a broader experimental study. This experiment is designed to address tasks of identification and control using predictive algorithms with a variable number of inputs and outputs. Fig. 1 shows the conceptual process schematic. The stand is based on a one-dimensional array of 25 electromagnets. These electromagnets are connected to an intermediate electronic board, a PWM-to-DC converter. This board receives a PWM signal from the Nucleo STM32H7 board, running custom software developed by the authors.

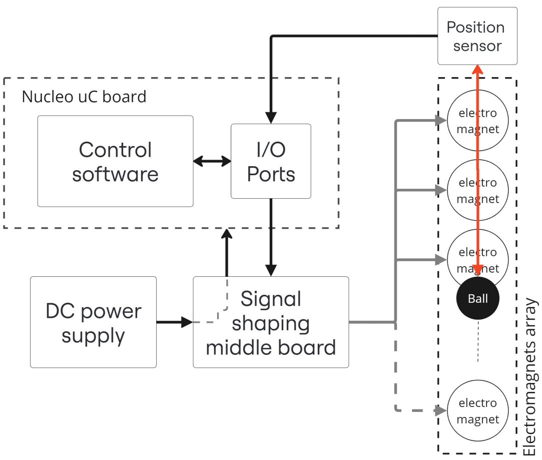

Fig. 1. The conceptual process schematic

The software controls the current of each electromagnet by regulating the voltage. Based on user-defined parameters and feedback from the position measurement sensor, the software utilizes predictive control algorithms to determine how many electromagnets should be engaged, which electromagnet should be powered on, and for how long. From a more abstract perspective, this system operates as a Single Input Multiple Output (SIMO) system with a dynamically changing number of outputs.

These tasks will be implemented to control the movement of a steel ball within a linear array of electromagnets. The entire system will be managed by an embedded system based on the STM32H7 family of processors without any assistance from external computational systems.

The process design assumptions are the following:

- the ball size is 0.017 m,
- the maximum ball velocity is 0.25 m/s,
- the track length is 0.5 m,
- the number of electromagnets is 25 units,
- the maximum sampling time is 0.02 ms,
- embedded systems only are considered to control and manage the process,
- the detector costs a maximum of 75 USD.

Fig. 2 depicts the process photo; the microcontroller and the power supply are also shown. The experimental setup has been constructed using 3D printing Fused Deposition Modeling (FDM) technology. The modular design of the track allows for changes in length and shape. Side barriers confine the motion of the ball. At the beginning of the track, there is a starting electromagnet with an inclined plane to impart initial velocity to the ball. A distance sensor is placed at the end of the track. Magnetic field visualization film is applied to the electromagnets, both as a visual representation of the magnetic flux and as a means to smooth the ball's rolling surface. Due to the manufacturing technique, the entire setup exhibits a tendency to bend into an arc. To mitigate this issue, the setup has been rigidly mounted onto an I-beam-shaped leveling base for structural stability.

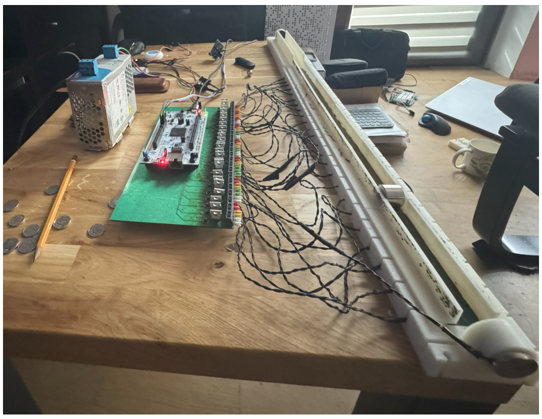

Fig. 2. The process (right), the microcontroller (middle) and the power supply (left)

The entire test software has been implemented in the C programming language, without the HAL libraries, and runs on an STM32H755 microcontroller. The microcontroller is connected to a dedicated electronic system with 25 channels.

Each channel can convert a PWM signal into a DC current proportional to the duty cycle of the input signal. Each channel is connected to a 3W electromagnet. The entire system is powered by a 24V power supply.

An an ultrasonic sensor has been selected for the experime for reasons described later in this worknts. The sensor is connected to the microcontroller via a General Purpose Input/Output (GPIO) interface, and each measurement is performed using the sequence depicted in Fig. 3.

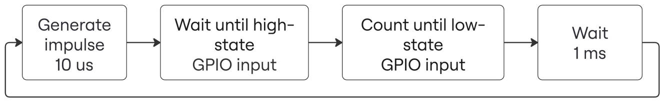

Fig. 3. Measurement Flow Chart

The prepared system is used to conduct research to identify the best method for distance measurement. The measurements can be divided into two types: static and dynamic. For the static measurements, the ball is stopped by successive electromagnets along its axis, and 100 measurements are taken for each of the 25 electromagnets. Since the ball and the electromagnets are not perfectly manufactured, it has been discovered during testing that the ball does not always stop at the same position. To address this issue, a form of pretensioning has been introduced into the system by elevating one end of the track, resulting in a 5-degree incline.

Dynamic measurements have also been conducted on the inclined track. At the beginning of the measurement, the ball is released by the starting electromagnet, and the tested sensor measures its position at the maximum available speed. Once the ball reaches a specified position, the sensor ceases measurements, and the results are transmitted via a serial port to a PC for further analysis.

III. Description of Possible Approaches to Position Measurement

Based on the boundary conditions of the experiment defined in Section II, a review of available technical solutions meeting the cost constraint has been conducted. Below is a summary of the most popular types of sensors, with a price not exceeding 100 USD.

A. Vision Distance Detectors

Vision sensors are among the most popular types of detectors. Numerous hardware and software solutions are available for image analysis. Their ease of use stems from the intuitive nature of interpreting results, as vision is the dominant sense for humans. An example parameter of an affordable camera that could meet the requirements is ArduCam Mini OV5642, shown in Fig. 4. It has the following properties:

- the maximum resolution is 2592 x 1944 px (5 MPx),
- the frame rate is up to 60 FPS for 720p format (1280x720 px),
- the lens size is 1/4",
- the pixel size is 1.4 x 1.4 μm,
- the image field size is 3673.6 x 2738.4 μm,
- the field of view is 24° (non-linear),
- the possible output formats are RGB565/555/444,
- the price is 50 USD.

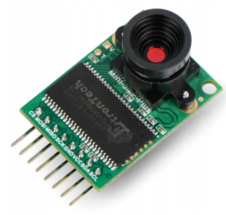

Fig. 4. ArduCam Mini OV5642

The camera's technical specifications suggest it could serve as a distance measurement system. However, a deeper analysis reveals structural obstacles to its application. Firstly, due to the focal length and sensor size, only a portion of the image would be analyzed for positions of the ball farther away from the camera. Consequently, resolutions around 720p must be transmitted to ensure sufficient detection resolution at greater distances. These images would then require extremely fast and complex processing to determine the distance. Considering that a 720p frame in RGB565 encoding is approximately 1.7 MB of data per frame, the processing time on STM32H7 systems would significantly exceed the 20 ms constraint. For these reasons, this solution has been rejected early in the evaluation process.

B. Laser Distance Detectors

Another interesting and inexpensive solution involves systems based on laser beams. Fig. 5 shows an example of commercial implementation of such an approach. The principle of operation relies on measuring the time it takes for light to return after reflecting off an obstacle. While these systems do not have the drawbacks of vision-based systems, such as high computational power requirements, their resolution is limited, and measurement uncertainty is high due to the speed of light. Lidar TF Luna sensor has the following properties:

- the operating range is 0.2 m to 8 m (90% reflectivity),
- the accuracy is $\pm$6 cm (from 0.2 m to 3 m),
- the resolution is 1 cm,
- the light resistance is up to 70 klux,
- the field of view is 2°,
- the price is approximately 30 USD.

Despite the many advantages of laser sensors, this type of detector has also been rejected due to the insufficient resolution and high measurement uncertainty of TOF sensors.

Fig. 5. Lidar TF Luna sensor

C. Capacistance and Resistance Touch Sensors

Another type of position sensor considered is the pressure sensor. These sensors perform exceptionally well in many positioning scenarios. They are simple, fast, and precise. Unfortunately, they cannot be applied when electromagnets are used to generate force acting on the ball. The attractive force of the electromagnet decreases significantly as the ball's distance from its surface increases. Even setting aside the critical issue of the absence of an off-the-shelf solution for the specific object being developed in this study, the presence of a pressure plate would significantly weaken the system's ability to control the process.

D. Acoustic Distance Sensors

The final and winning solution is the acoustic distance detector. Fig. 6 illustrates two commercial implementations of such sensors. A side-by-side configuration is shown on the left. The transmitter and receiver are placed next to each other. A coaxial configuration is depicted on the right. The transmitter and receiver are housed within a single unit. The sensor HC-SR04 (side-by-side sensor) has the following properties:

- the measurement speed is 15 ms,
- the measurement range is 2-400 cm,
- the resolution is 3 mm,
- the measurement time is 150 μs-25 ms,
- the emission angle is 15°,
- the price is 5 USD.

The sensor JSN-SR04T-V3.0 (coaxial sensor) has the following properties:

- the probe frequency is 40 kHz,
- the range is 20-600 cm,
- the uncertainty (for long range) is $\pm$1 cm,
- the resolution is 1 mm,
- the angle is 75°,
- the price is 10 USD.

Fig. 6. Examples of ultrasonic sensors: side-by-side (left) and coaxial (right)

The manufacturer's data clearly shows that the acoustic sensor offers significant advantages over its predecessors. These features make it the first choice for initial attempts at implementing distance measurement. Let us name the most important advantages of acoustic distance sensors:

1) High resolution and low measurement uncertainty. Using acoustic waves significantly slower than light, inexpensive ultrasonic sensors based on time-of-flight measurement can determine the position and its changes more precisely than affordable laser sensors.
2) Simplicity of implementation and measurement speed. The sensor requires only two GPIO pins and one timer for operation. Both blocks are hardware-implemented in microcontrollers, and their handling takes just a few clock cycles.
3) Immunity to magnetic phenomena. The nature of acoustic waves allows for readings in environments with fluctuating magnetic fields.
4) No impact on the magnetic field. The measurement does not reduce the electromagnetic force acting on the rolling object in any way.
5) Extremely low cost. The sensor is far cheaper than most alternatives.

Despite the significant advantages named above, the considered sensor also has several important drawbacks stemming from the nature of acoustic phenomena:

1) Uncontrolled propagation of sound waves. Acoustic waves spread in all directions, resulting in the receiver detecting not only waves reflected from the target object but also those reflected from other obstacles. This means that a changing environment can impact measurement repeatability.
2) Resonance phenomena. Due to the specific wavelength of acoustic waves, resonance can occur between two reflective surfaces at certain distances. This can lead to signal amplification or attenuation at specific measurement points, resulting in inaccurate distance readings.
3) Decreasing resolution and increasing measurement time with distance. While the limited speed of acoustic waves enables reasonable measurement accuracy, it also becomes a drawback at greater distances. Points farther from the sensor are measured more slowly, increasing the distance traveled between measurements and reducing resolution.
4) Measurement offset caused by temperature and humidity. As temperature and humidity change, the speed of sound also changes, causing measurement readings to shift by several millimeters. This can significantly impact the accuracy of the experiments conducted.

This work describes a series of studies aimed at minimizing the above-mentioned limitations. The experiments have been designed to determine the ranges of measurement uncertainty, minimize these uncertainties, and establish the feasibility of using the acoustic sensor in the final experimental setup. The findings provide insight into overcoming these challenges and leveraging the sensor's strengths for accurate and reliable measurements.

IV. Physics Behind the Acoustic Position Sensors

Every ultrasonic sensor is based on simple physical principles. The transmitter emits a sound wave at a frequency of f = 40 kHz, which is well above the human hearing range, typically between 20Hz and 20kHz [16]. At the moment the wave is emitted, a timer is started. This timer is stopped by the receiver when it detects the wave reflected from an obstacle. Based on the measured elapsed time and knowing the speed of sound in air, which is around 350m/s [17], it is possible to determine the distance between the transmitter and the obstacle. Of course, the speed of sound is not a strictly constant value; it depends on temperature and air humidity [17]. Consequently, for accurate distance measurements, in addition to measuring the time of the reflected wave's arrival, one also needs to account for the atmospheric conditions in which the acoustic wave propagates.

This is essentially where the simplicity ends, and more complex phenomena begin. If sound behaved like a laser beam, the analysis of reflections would be straightforward. However, sound behaves more like water, spreading out in all directions immediately after emission. As a result, a complex acoustic field is generated, whose time-varying shape results from the superposition of reflected waves of different amplitudes and phases [17]. For signal detection quality, such features of the acoustic field as acoustic background noise, the presence of strong reflections, diffraction, and interference of acoustic waves are significant [16], [18].

In the case of acoustic background noise, the problem is not very significant because there are few sound sources in the human environment operating in the 40 kHz range used by the sensor. On the other hand, reflections from objects other than the intended target can substantially affect the measurement, introducing interference. If the difference in acoustic pressure levels between the target reflection and the interfering reflection is less than 3 dB, the receiver may interpret the reflected wave incorrectly. Even though sound absorption in air increases substantially with frequency [16], this phenomenon is not intense enough to ignore reflections from nearby objects. Therefore, it is crucial to keep the space around the sensor free of interfering elements.

Acoustic resonance is another important phenomenon resulting from multiple reflections in a closed, reflective space. Acoustic resonance, or the formation of standing waves, leads to a non-uniform, spatially varying acoustic field. Standing waves arise from interference between acoustic waves—through their mutual reinforcement or cancellation [16]. This non-uniform acoustic field that forms at certain distances from the sensors can effectively limit the possibility of making accurate measurements in certain regions around the sensor.

V. Practical Evaluation of Acoustic Position Sensors

After deploying the sensor on the test setup, the initial experiments have been conducted in accordance with the methodology described above. The obtained results are surprisingly promising. There are several distance ranges where the readings are accurate. Unfortunately, there are also ranges where the discrepancy between the measured and actual positions exceeds 20 mm. Additionally, there are locations where the readings are completely incorrect or absent altogether.

The most significant drawback of the applied method is the extreme variability in the characteristic of the measured deviations from the actual position. As a result, no universal correction could be applied because, for reasons unknown at the time, a correction that worked for one series of measurements proved completely inaccurate for others.

More than 250,000 measurements have been performed in various configurations to identify the sources of these deviations. A selection of these measurements, along with their conclusions, is described in Section V-A.

A. Measurement Improvement Tested Methods

After obtaining the initial research results, which turned out to be surprisingly promising, efforts have been made to improve the elements that significantly fell short of the requirements. Particularly problematic are the substantial deviations of the measured position from the expected position. Errors in position detection of a magnitude comparable to the diameter of the electromagnet would render the sensor unsuitable for controlling the ball's rolling process.

However, the fact that the large errors are confined to narrow intervals suggests the possibility of eliminating or reducing the existing anomalies. To this end, a series of static tests have been conducted, and the results are presented in Section V-C. It has been initially hypothesized that the existing problems resulted from acoustic resonances described in Section IV. Due to the lack of appropriate equipment for ultrasonic wave measurements, experimental actions have been taken based on the author's extensive acoustic experience spanning over a decade.

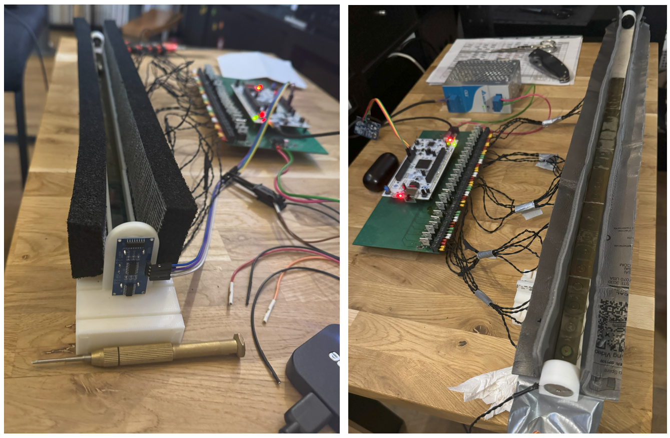

Fig. 7. Elastic bands (right) and acoustic absorber (left) as a part of trial-and-error measurement improvement process

1) Measurement Stand Band Changes: The first action taken has been the installation of soft, absorbing covers as extensions of the barriers along which the ball rolls. Fig. 7 shows the stand with the tested bands. For acoustic phenomena, reflections from surrounding elements have a significant impact. The sensor has an emission angle of several degrees, meaning that it detects waves reflect from the target object and interfering waves reflect from elements in the environment. Naturally, a solution that limits the interfering waves reaching the receiver would significantly reduce measurement uncertainty. An additional benefit would be the partial or complete elimination of resonance between the barriers, which could also contribute to local disturbances.

Unfortunately, the tests show that both types of acoustic sensors stopped functioning entirely. Connecting a logic analyzer revealed a complete lack of detection of reflected signals.

The conclusion is straightforward: the barriers are so absorbent that, given the transmitter's low power, the wave either fails to reach the target object or lacks sufficient acoustic energy to return to the receiver and be detected by the sensor. Increasing the power of the emitted acoustic wave would likely solve the problem, but this is not a feasible option in the current setup.

The second attempt involves replacing the rigid plastic barriers with the attached acoustic foam and replacing them with flexible, easily shapeable barriers. For this purpose, a medical splint commonly used for stabilizing fractures, known as a Kramer splint, is utilized. This splint is an aluminum flat core covered with approximately 3 mm of closed-cell foam. The splint's flexibility allows for free shaping, which raised the hope of forming it in a way that would eliminate any resonant disturbances. The closed-cell foam covering also provided sound-damping properties, albeit much lower than the previous solution.

In practice, however, manually shaping the barriers to achieve precise control over the propagation of acoustic waves proves impossible without additional specialized equipment. The results become even less precise, and in some cases, the sensors stop functioning altogether.

The next attempt involves creating high barriers, twice the height of the measured ball, using 3D printing, and replacing the low barriers with higher ones. The goal was to minimize the influence of reflected waves on the measurement by blocking them as much as possible. Unfortunately, the measurements show no significant improvement, so the idea has been abandoned. Additionally, the high barriers impede visual observation of the setup, further reducing their practicality.

The improvements achieved so far have not been satisfactory. During subsequent hundreds of measurements to find a method to improve positioning accuracy, it is observed that the tilt angle of the barriers relative to each other and the gap between the barriers and the measured object significantly influenced the results. For example, a large gap between the ball and the barriers or barriers arranged parallel to each other causes substantial measurement disturbances and produces incorrect positioning results.

One key conclusion from these observations is that any changes in the arrangement or position of the barriers between measurement series cause a complete loss of correlation between the distance from the sensor and the measurement deviation from the actual position.

Through trial and error, it has been determined that tilting the barriers at a small angle of approximately 3 degrees and fixing them securely in place results in satisfactory improvement. Tilting the barriers by a few degrees lowers the acoustic field inhomogeneity and increases the measurement accuracy. Additionally, commonly available gray fabric-reinforced duct tape has been applied to the barriers to reduce the impact of barrier joints and increase their acoustic absorption.

2) Measurement Stand Environment Changes: The impact of the operator's presence and obstacles near the experimental setup has been also examined during the tests. The conclusion in this case is as expected: the presence of reflective elements near the sensor, e.g., the presence of the operator's hand or a wall causes immediate measurement disturbances. Sometimes, measurements across the entire track length become impossible, while only certain sections are affected at other times. The presence of additional reflections is immediately evident in the results. Occasionally, moving the setup by just a few centimeters causes a dramatic drop in detection quality. As shown in Fig. 10, the setup, located near a wall in this case, is protected from reflections by placing acoustic foam (visible as pink foam on the left side).

3) Sensor Changes: As shown in Fig. 6, two sensor configurations have been tested to evaluate various ultrasonic sensor designs regarding measurement accuracy and resistance to interference. Additionally, to ensure the repeatability of results, each sensor type is tested using two individual units. The conducted tests reveal differences between the sensor types, but no significant discrepancies are observed between units of the same type.

The primary difference between the sensor types is the superior resistance of the coaxial sensor to external interference. This is evident in the significant decline in measurement accuracy towards the end of the track for the "side-by-side" sensors. This effect is clearly visible in Fig. 8, where the measurement error increases noticeably, and some readings are even lost at the far end of the measurement range.

Furthermore, the side-by-side sensor is highly sensitive to changes in the tilt angle. This sensor also exhibits larger deviations from actual values, making it less precise and less repeatable. All mentioned characteristics lead to the selection of the coaxial sensor for further dynamic testing.

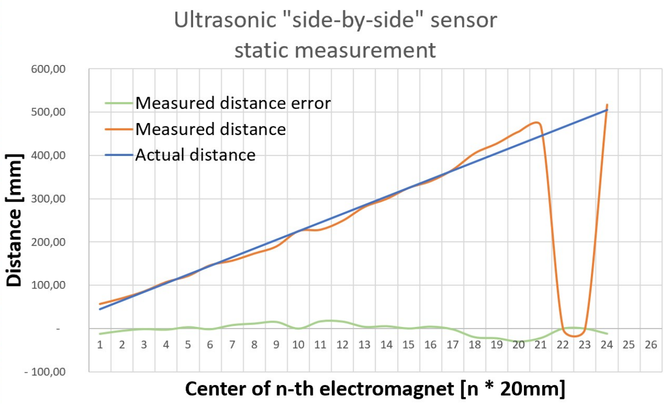

Fig. 8. Initial position measurement graph: The loss of samples and the low accuracy level are clearly visible

4) Measured Object Changes: During the research, the tested object itself has been analyzed. Initially, it is a 12 mm diameter bearing ball. It has been decided to verify how changing the diameter or shape of the rolling element would affect measurement quality. Balls with diameters of 12 mm, 15 mm, 17 mm, and 20 mm, as shown in Fig. 9, and a 20 mm diameter roller have been tested.

The conclusion is as expected: larger balls and the roller provide greater stability in readings. Since there are no significant differences between the 17 mm and 20 mm balls, the 17 mm ball has been chosen for practical reasons. The roller, which also performs well during the test measurements, has been excluded for practical reasons. Unlike the balls, the roller occasionally becomes stuck against the barriers, making it unsuitable for further experiments.

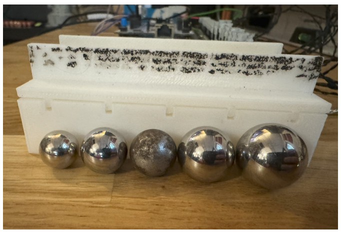

Fig. 9. The tested balls

5) Repeatable Position Improvements: The final structural element considered has been the surface on which the ball rolls. An intermediate leveling layer is necessary since the electromagnets create an uneven surface. This layer is needed to minimize the reduction of the electromagnetic force acting on the ball while providing a smooth surface.

After testing various solutions, a magnetic field detection film has been ultimately selected. This film is thin and rigid enough to meet the requirements and changes color when a specific electromagnet is active. This last feature proves invaluable for visual inspection and evaluation of the behavior of the programmed algorithms.

6) Final Test Hardware Setup: Fig. 10 presents the final test configuration. The barriers fixed at a slight angle and covered with the film are depicted. The magnetic field-sensitive film adheres to the electromagnets, and the coaxial ultrasonic sensor is visible at the end of the setup. The results presented next have been obtained using this configuration.

Fig. 10. The final version of the test stand; tape glued to the fixed bands, sidewall acoustic foam and rolling magnetic sensitive foil

B. Side-By-Side Type Static Measurements

During the initial test setup operation, measurements are performed using the “side-by-side” sensor. In the first tests, several measurement series are conducted, during which 5 samples are recorded for each of the 25 electromagnets. The results of two such series are presented in Fig. 11. As can be seen in the figures, the initial results exhibit significant scatter compared to the actual values. In the first sub-figure, there is a 200 mm drop at the position of the 18th electromagnet and 100 mm drop at the position of the 20th electromagnet. In the second sub-figure, there is a 60 mm drop at the 22nd electromagnet. Additionally, there are substantial differences between individual series. The overall impression is one of high randomness in the variations. As it is later discovered, this randomness results from the simultaneous influence of several variables, whose random fluctuations create the appearance of complete unpredictability.

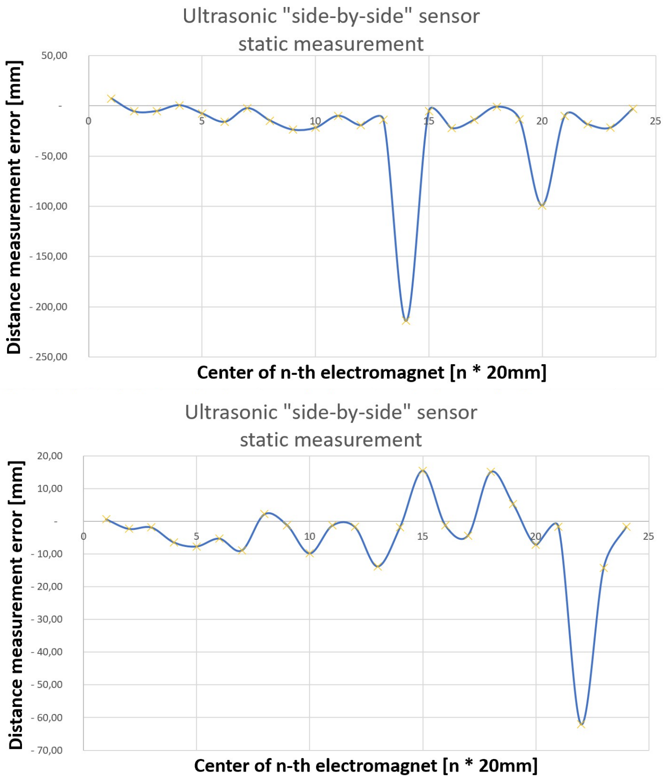

Fig. 11. Static measurements; significant measurement errors are clearly visible

Despite the challenges mentioned above, it has been decided to pursue optimization methods due to the significant advantages of the acoustic measurement method, as described in Section III-D. The entire optimization process is detailed in Section V-A, and its outcomes are presented below.

C. Coaxial Type Static Measurements

Due to the significant discrepancies between the series, a sensor with a different design has been implemented. A coaxial sensor, fully shielded by the barriers, has been installed. This optimization process is described in Section V-A3. Additionally, the software has been restructured to enhance its automation. As a result, during the first tests with the new configuration, 10 measurement series are conducted, each recording 100 samples for each of the 25 electromagnet positions. In total, 25,000 samples are collected during the first experiment. The collected measurements are summarized in Fig. 12. Dozens of such experiments are performed.

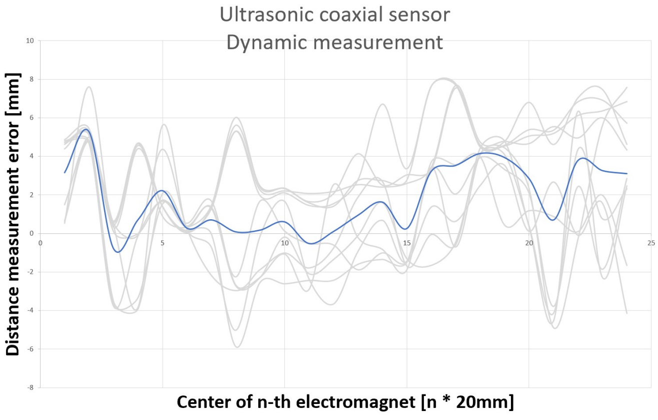

Fig. 12. Static measurements taken with a coaxial ultrasonic sensor

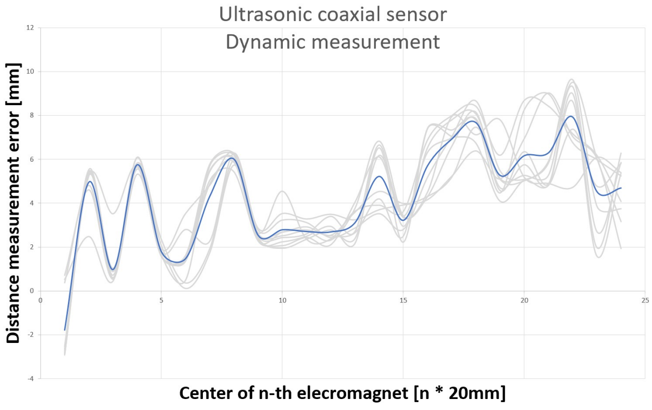

Fig. 13. Static measurements taken with a coaxial ultrasonic sensor after applying several optimizations

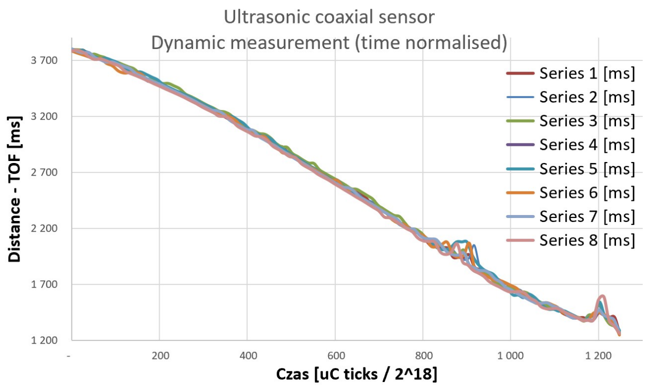

Fig. 14. Dynamic measurements taken with a coaxial ultrasonic sensor

The research results are very promising. Although, as shown in Fig. 12, there is significant variability between series, all deviations in the measured positions fall within a range of a few millimeters.

During the course of numerous experiments, an intriguing phenomenon is observed. Series collected on the same day tend to be consistent, while data gathered the following day often exhibited completely different deviation patterns. This "next-day effect" is consistent for samples collected on that day but entirely different from the patterns observed on the previous day. There are also instances where 6 out of 10 series show strong similarity, while the remaining 4 are markedly different.

These observations described above encouraged us to identify the causes of this phenomenon, which are discussed in detail in Section V-A. Determining the reasons for the lack of consistent patterns has been critical because maintaining stable deviation profiles across all series would enable straightforward application of correction methods, such as using neural networks.

The outcome of the series of optimizations described in Section V-A, along with hundreds of thousands of measurements, is presented in Fig. 13. Minimal deviations and remarkable repeatability of the patterns are clearly shown, enabling the application of corrective algorithms and achieving precise results.

Let us stress that the described results are obtained using a sensor costing only 10 USD, with negligible computational power requirements and within a processing time of 17 ms. The results exceed even the expectations of the authors of this study.

D. Coaxial Type Dynamic Measurements

After conducting extensive static tests, the next step is evaluating the sensor's dynamic measurement capabilities. There is a non-zero probability that a sensor performing excellently in static measurements might fail to operate correctly when measuring a moving ball. On the other hand, the authors are also interested in determining the extent to which local irregularities observed in static measurements would be reflected in dynamic measurements.

As with the static measurements, multiple series of dynamic measurements have been performed. The measurement presented in Fig. 14 shows the results of eight measurement series without applying time normalization. At first glance, it is evident that the patterns have a similar character but are shifted by several tens of milliseconds relative to each other.

Whether these differences result from variations in the ball's rolling path or inconsistencies in the ultrasonic sensor's signal processing time is not further investigated. However, efforts have been made to align the timing of the collected patterns. The result of this time normalization is presented in Fig. 15.

As shown in Fig. 15, the measured positions of the ball during its motion along the inclined plane are very consistent. All eight trajectories exhibit localized intervals of increased deviation from the expected position, corresponding to the ball's motion along the incline. These intervals are located around 900 ms and 1200 ms on the plot. This high degree of consistency across the trajectories offers a promising opportunity to implement a correction system to reduce measurement uncertainty.

Figs. 16, 17 and 18 present magnified sections of Fig. 15, divided into three parts for detailed analysis. The first part, shown in Fig. 16, illustrates the measurement segment for the greatest distances from the sensor. The trajectories in this segment are consistent, with no visible local anomalies. Fig. 17

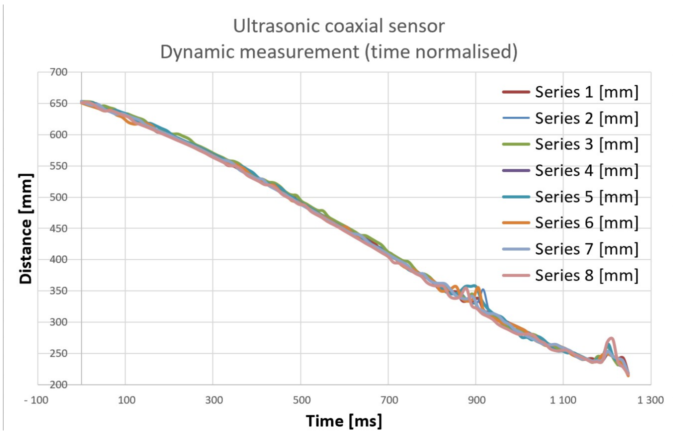

Fig. 15. Dynamic measurements taken with a coaxial ultrasonic sensor after normalization

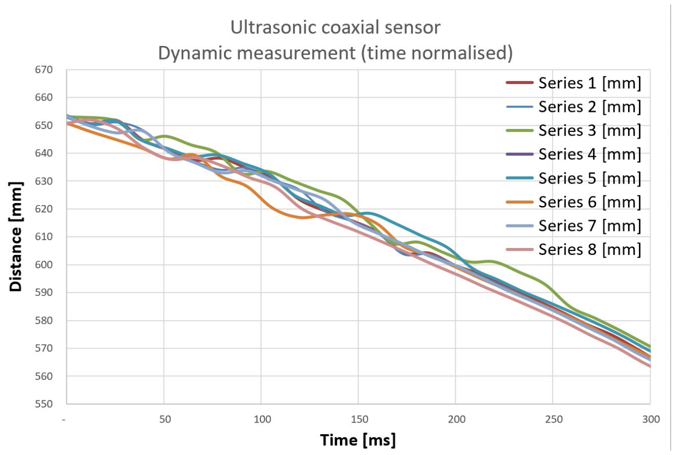

Fig. 16. Graph of dynamic measurements taken with a coaxial ultrasonic sensor after normalization; zoom boundaries: 0-300 ms

similarly shows consistent trajectories across the series. Only the final segment, closest to the sensor and depicted in Fig. 18, reveals two significant local deviations from the expected trajectories. These deviations may result either from acoustic resonance phenomena or from intrinsic characteristics of the sensor itself. At the time of writing this article, the exact cause of this phenomenon has not yet been determined. However, there is good news. The patterns of these disturbances, particularly around 1200 ms, are consistent, allowing for precise correction. Around 900 ms, the correction will be less precise but still feasible.

E. Improvements Achieved

The improvement in the obtained results is well illustrated by the significant reduction in deviations of individual measurement series from the mean of all series. Fig. 19 shows the average deviation from the overall mean value, calculated from all series, for each measured position.

The analysis of overlaid results before and after optimization clearly indicates a substantial improvement in measurement repeatability. A single numerical indicator, which is the sum of the average deviations of the measurement series from

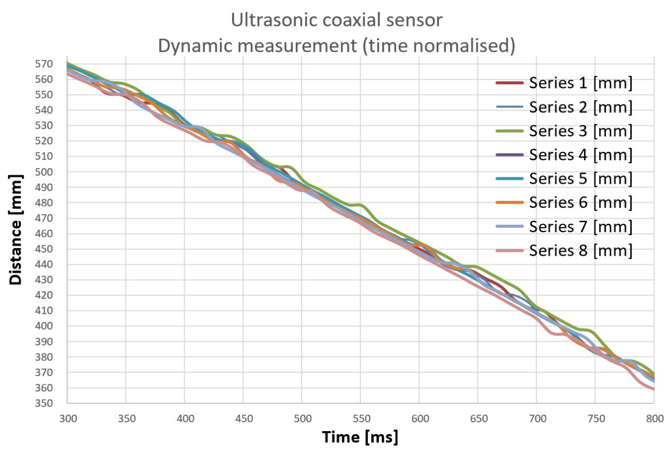

Fig. 17. Graph of dynamic measurements taken with a coaxial ultrasonic sensor after normalization; zoom boundaries: 300-800 ms

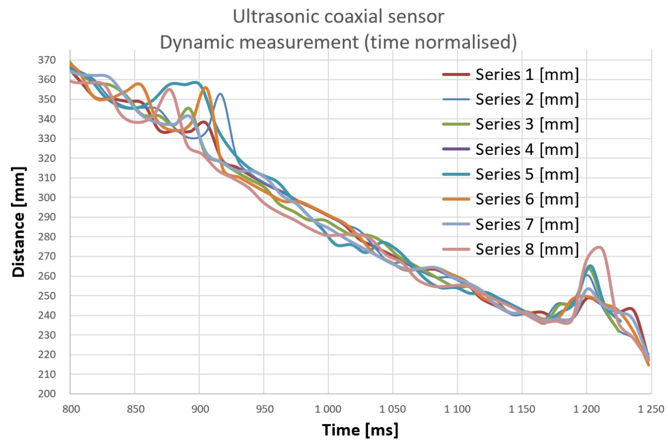

Fig. 18. Graph of dynamic measurements taken with a coaxial ultrasonic sensor after normalization; zoom boundaries: 800-1250 ms.

their overall mean value, shows a reduction of over 50% after optimization compared to before. Thus, all measurements are effectively much "closer" to the mean value than before optimization.

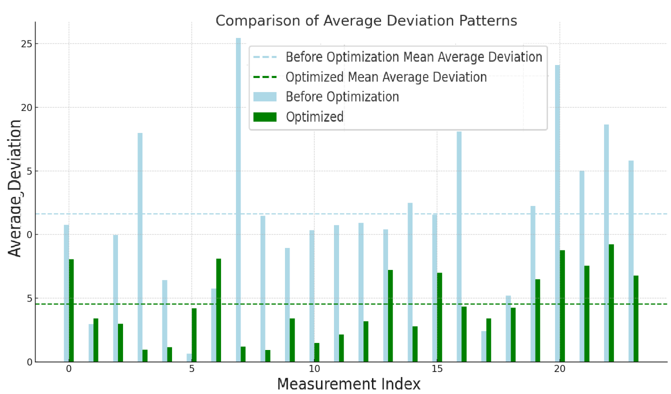

Fig. 19. The average deviations of measurement series from their mean values

VI. Conclusions

The presented research results clearly demonstrate the immense potential of acoustic sensors. Their advantages go beyond purchase and computational power costs, extending to the results' quality, even compared to relatively inexpensive laser sensors, which are still several times more expensive than ultrasonic sensors.

As a result of the work conducted and described, significant improvements in sensor readings have been achieved. In the initial phase, the measured distances deviate by several tens of millimeters from the actual values, as shown in Fig. 11. By the final stage, the sensor's measurement error is reduced to just a few millimeters, as illustrated in Fig. 13, representing an improvement by at least several times. The scale of this improvement is clearly depicted in Graph 19. Furthermore, the applied changes eliminate instances where the sensor failed to provide measurement results.

However, like any other method, acoustic technology has its limitations. The most problematic factors include the effects of acoustic resonances, reflections from objects nearby, and the influence of acoustic background noise from external sources, all described in Section IV. Each of these factors can significantly impact the feasibility of implementing ultrasonic distance sensors, potentially making their use impractical in certain conditions. On the other hand, skillfully managing these drawbacks can turn this technology into a highly effective tool for various applications.

Although the results are good, they do not exhaust the available possibilities. The most promising research direction now appears to be exploring the potential for rapid software-based correction of static and dynamic results to mitigate local measurement deviations. Another intriguing step would be investigating the implementation of an auto-tuning function that accounts for temperature and acoustic background measurements, enabling the measurement system to operate independently of external environmental conditions.

Furthermore, access to appropriate equipment might make it possible to modify existing sensors or even develop a customized solution tailored to specific implementation requirements.

References

[1] L. D. Feisel and A. J. Rosa, "The role of the laboratory in undergraduate engineering education," *Journal of Engineering Education*, vol. 94, pp. 121–130, 2004.
[2] "Bytronic," https://www.bytronic.net/product-category/control-systems/.
[3] "Inteco," http://www.inteco.com.pl/.
[4] "Quanser," https://www.quanser.com/.
[5] "Automation shield: Control systems engineering education," https://github.com/gergelytakacs/AutomationShield/wiki.
[6] G. Takács, E. Mikuláš, M. Gulan, A. Vargová, and J. Boldocký, "Automationshield: An open-source hardware and software initiative for control engineering education," *IFAC-PapersOnLine*, vol. 56, pp. 9594–9599, 2023, 22nd IFAC World Congress.
[7] G. Takács, J. Mihalík, M. Gulan, A. Vargová, E. Mikuláš, and Š. Ožana, "Magnetoshield: A novel open-source magnetic levitation benchmark device for mechatronics education and research," *Sensors*, vol. 24, p. 538, 2024. [Online]. Available: https://www.mdpi.com/1424-8220/24/2/538
[8] E. Chołodowicz and P. Orłowski, "Low-cost air levitation laboratory stand using MATLAB/Simulink and Arduino," *Pomiary Automatyka Robotyka*, vol. 21, pp. 33–39, 2017.
[9] R. M. Reck and R. S. Sreenivas, "Developing an affordable and portable control systems laboratory kit with a raspberry Pi," *Electronics*, vol. 5, p. 36, 2016.
[10] A. Wojtulewicz, P. Chaber, and M. Ławryńczuk, "Multiple-input multiple-output laboratory stand for process control education," in *2016 21st International Conference on Methods and Models in Automation and Robotics (MMAR)*, 2016, pp. 466–471.
[11] K. Zarzycki and M. Ławryńczuk, "Fast real-time model predictive control for a ball-on-plate process," *Sensors*, vol. 21, no. 12, p. 3959, 2021. [Online]. Available: https://www.mdpi.com/1424-8220/21/12/3959
[12] G. C. Goodwin, A. M. Medioli, W. Sher, L. B. Vlacic, and J. S. Welsh, "Emulation-based virtual laboratories: A low-cost alternative to physical experiments in control engineering education," *IEEE Transactions on Education*, vol. 54, pp. 48–55, 2011.
[13] V. Potkonjak, M. Gardner, V. Callaghan, P. Mattila, C. Guetl, V. M. Petrović, and K. Jovanović, "Virtual laboratories for education in science, technology, and engineering: A review," *Computers & Education*, vol. 95, pp. 309–327, 2016.
[14] M. Kalúz, Ľuboš Čirca, R. Valo, and M. Fikar, "Arpi lab: A low-cost remote laboratory for control education," *IFAC Proceedings Volumes*, vol. 47, pp. 9057–9062, 2014, 19th IFAC World Congress.
[15] S. C. McLoone and J. Maloco, "A cost-effective hardware-based laboratory solution for demonstrating PID control," in *2016 UKACC 11th International Conference on Control (CONTROL)*, 2016, pp. 1–6.
[16] K. C. P. F. Alton Everest, *Master Handbook of Acoustics*. McGraw-Hill, 2021.
[17] T. D. Rossing, *Springer Handbook of Acoustics*. Springer, 2007.
[18] P. Newell, *Recording Studio Design*. Focal Press, 2008.